883 IMPACT OF HIGH RESOLUTION ELEVATION AND LAND USE DATA ON SIMULATED CONVECTIVE ACTIVITY OVER CENTRAL GREECE

Stergios Kartsios*, Theodore Karacostas, Ioannis Pytharoulis, Ioannis Tegoulias, Stelios Kotsopoulos and Dimitrios Bampzelis
Department of Meteorology and Climatology, Aristotle University of Thessaloniki, Greece

1. INTRODUCTION

During last years the need of ingesting high resolution data into numerical weather prediction (NWP) models is emphasized, in order for physical processes to be represented in most accurate way. On the other hand, the development of new sophisticated atmospheric models, in conjunction with modern instruments for recording and measuring atmospheric and cloud physics data have increased the interest for weather modification, and particularly for precipitation enhancement projects (Silverman 2003).

In the framework of project DAPHNE, the agricultural drought in Thessaly plain is being assessed by means of Weather Modification (Karacostas et al. 2014). The main objective of the project is the development of necessary scientific tools to support the potentiality and applicability of a well-designed precipitation enhancement program. The region of Thessaly in central Greece is the most vital agricultural area of the country, where climate change, population increase and continuous exhaustion of water reservoirs have amplified the already existed problem of drought, which has prevailed during several years of the last decades.

The aim of this study is to investigate the impact of very high spatial resolution topography and land use data in the characteristics of convective activity, over Thessaly plain. The non-hydrostatic Weather Research and Forecasting model with the Advanced Research dynamic solver (WRF-ARW, version 3.5.1) is initialized under different synoptic conditions in central Greece and is evaluated against available radar data and surface observations.

Corresponding author address: M.Sc. Stergios Kartsios, Dept of Meteorology and Climatology, School of Geology, Faculty of Sciences, Aristotle Univ. of Thessaloniki, 54124 Thessaloniki, Greece;
e-mail: kartsios@geo.auth.gr

2. DATA AND METHODOLOGY

The non-hydrostatic WRF-ARW model (Skamarock et al. 2008, Wang et al. 2013) was utilized for the purposes of this study. The model is integrated in three domains, using 2-way telescoping nesting which cover Europe, the Mediterranean Sea and northern Africa (d01), the wider area of Greece (d02) and central Greece – Thessaly region (d03), at horizontal grid-spacings of 15km, 5km and 1km respectively (Fig. 1). ECMWF operational analyses at 6-hourly intervals (0.25°x0.25° lat.-long.) were imported as initial and boundary conditions for the coarse domain. Each hindcast had a time horizon of 36 hours and was initialised twelve (12) hours before each day of interest. The SSTs were provided by NCEP at a horizontal increment of 1/12°x1/12° lat.-long. and remained fixed to the initial values throughout the forecast horizon. In the vertical, all nests employed 39 sigma levels (up to 50 hPa) with increased resolution in the boundary layer. Microphysical processes were represented by WSM6 scheme, sub-grid scale convection by Kain-Fritsch scheme, longwave and shortwave radiation by RRTMG scheme, surface layer by Monin-Obukhov (MM5), boundary layer by Yonsei University and soil physics by NOAH Unified model.

Furthermore, high resolution (3'') elevation data from Shuttle Radar Topography Mission (SRTM – v4, Jarvis et al., 2008) were inserted in the innermost domain (d03) along with Corine Land Cover 2000 (Bossard et al., 2000) raster data (3''x3'', v.17). Corine land cover data were reclassified into USGS land use categories following Pineda et al. (2004), as depicted in Fig. 2.

Previous studies examined a series of model configurations through sensitivity runs (Tegoulias et al. 2014) and compared the characteristics of the simulated convective activity over Thessaly against radar data (Pytharoulis et al. 2014). The day with the best scores (ME,MAE) from each one of the six (6) upper-air synoptic circulation types (Karacostas et al., 1992), presented in

Pytharoulis et al. (2014), was selected in order to ingest the high resolution elevation and land use data into WRF model. The 6 upper-air synoptic circulation types which describe the prevailing conditions in Greece and used in this work, are: 1) zonal flow (ZON), 2) northwest flow (NW), 3) closed low (CLO), 4) cut-off low (CUT), 5) southwest flow (SW), 6) open trough (L1).

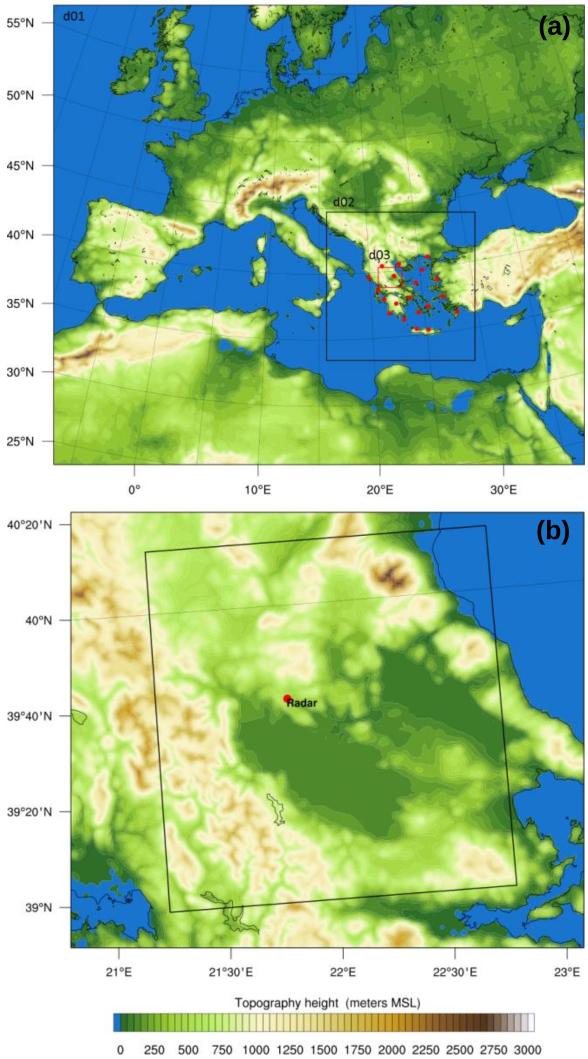

Fig. 1. The topography of (a) the coarse domain – d01 and (b) the innermost – d03 nest used by WRF. On panel (a), d02 (black frame) and d03 (red frame) are illustrated. The utilized HNMS stations are indicated in red. On panel (b), Radar denotes the location of the weather radar while the black frame over Thessaly encompasses the region with radar data.

Therefore, for each representative day, four (4) different model configurations were designed. The tUSGS-lUSGS configuration acted as the CONTROL experiment, where in the innermost domain (d03), the topography and land-use variables were represented by the USGS dataset (30'). In the tSRTM-lCORINE simulations, the topography and land use variables were described by the SRTM elevation data (3'') and the Corine raster data (3'') respectively in d03. The tSRTM-lUSGS and tUSGS-lCORINE configurations were used in order to investigate the impact of each dataset to the moist convection over the area of interest.

Moreover, statistical evaluation was carried out in d02 (wider area of Greece), using available surface observations from twenty (20) stations of the Hellenic National Meteorological Service (HNMS). The resulting errors were investigated as a function of the four (4) different model configurations, described above.

In addition, the maximum reflectivity in the column, the area and the volume of convective activity, the cloud top and cloud base were examined. The analysis was performed at the innermost domain (d03). Convective activity was considered to occur at the locations where the maximum reflectivity of the column, in the model or radar data, was higher than 35 dbz (Pytharoulis et al. 2014). The cloud base and cloud top were estimated as the lower and upper heights (inside the cloud) where the reflectivity was greater than 35dbz. The same threshold was applied for the area and the volume of convective activity. It must be mentioned that at each model output time, (every 10 min) the total activity, and not each individual convective cloud, was considered.

The aforementioned analysis was performed on a 140km x 140km region (Fig. 1b) because it includes most of Thessaly and is covered by the C-Band (5cm) weather radar of Liopraso (39.674°N, 21.837°E; Fig. 1b), interfaced to TITAN (Thunderstorm Identification, Tracking, Analysis, and Nowcasting) (Dixon and Wiener, 1993) for data analysis. Instantaneous model and radar data were transformed to hourly values by considering the maximum reflectivity, maximum cloud top and average cloud base, average area and volume, at each hourly period of every selected day. Data analysis and visualizations were done using the NCAR Command Language (NCL-v6.1.0), while the Model Evaluation Tools (METv4.1) was used for the statistical evaluation of the model performance.

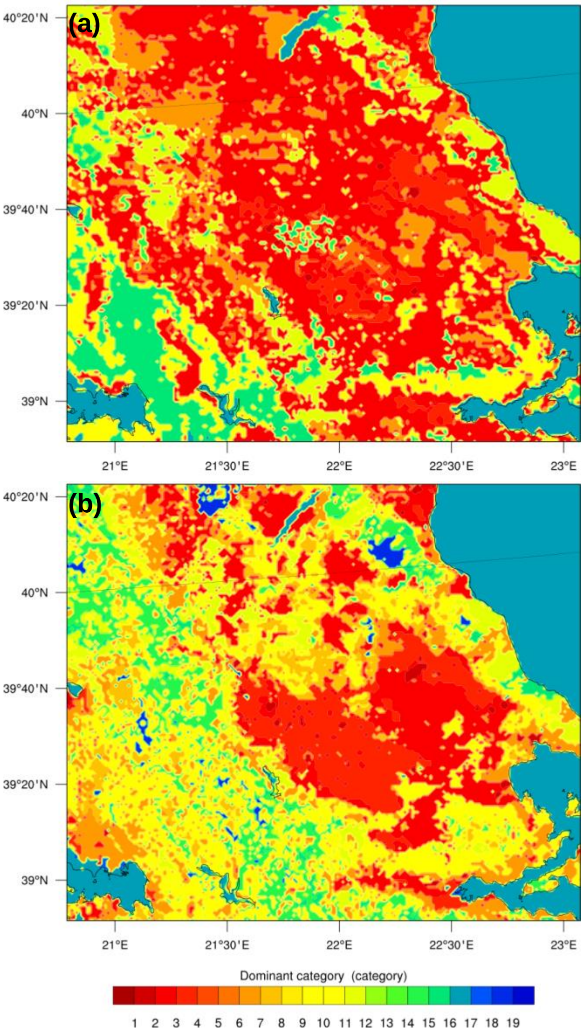

Fig. 2. Land use category classes in d03 according to USGS classification. Panel (a) depicts the USGS dataset while panel (b) shows the Corine data, reclassified into USGS land cover data. Categories are as follow, 1-Urban and built-up land, 2-Dryland cropland and pasture, 3-Irrigated cropland and pasture, 4-Mixed dryland/irrigated cropland and pasture, 5-Cropland/grassland mosaic, 6-Cropland/woodland mosaic, 7-Grassland, 8-Shrubland, 9-Mixed shrubland/grassland, 10-Savanna, 11-Deciduous broadleaf forest, 12-Deciduous needleleaf forest, 13-Evergreen broadleaf, 14-Evergreen needleleaf, 15-Mixed forest, 16-Water bodies, 17-Herbaceous wetland, 18-Wooden wetland, 19-Barren or sparsely vegetated.

3. RESULTS

3.1 Statistical evaluation at d02

For the statistical evaluation of the WRF performance, as a function of the four (4) different model configurations, the fields of mean sea-level pressure (MSLP), 10m wind speed, (WIND), 2m air temperature (TEMP) and 2m relative humidity (RH) are evaluated in d02 at the locations of the twenty (20) available HNMS stations (Fig. 1a). The first twelve (12) forecast hours are not considered, as we are interested only in each representative day.

Table 1 shows the Mean Error (ME) of mean sea-level pressure (hPa), air temperature (K), relative humidity (%) and wind speed (m/s). The model clearly underestimates MSLP and TEMP variables, while overestimates the RH and WIND parameters at all four (4) configurations. It should be emphasized that the differences occur mostly at the second decimal, indicating that the changes in topography and land-use at d03, affect the overall forecast at d02 in a minor way.

Table 1. Mean Error (ME) of mean sea-level pressure (hPa), air temperature (K), relative humidity (%) and wind speed (m/s) at d02 for each model configuration.

	MSLP ME	*TEMP ME*	*RH ME*	*WIND ME*
tUSGS-lUSGS	-0.761	-0.541	5.072	0.924
tSRTM-lUSGS	-0.76	-0.538	5.01	0.933
tUSGS-lCORINE	-0.765	-0.527	4.945	0.922
tSRTM-lCORINE	-0.762	-0.53	4.957	0.924

Fig. 3 depicts the Mean Absolute Error (MAE) of MSLP and RH (a), TEMP (b) and WIND (c) at d02, for each model configuration. Although there are minor differences between configurations, for the MSLP and TEMP variables, the tSRTM-lUSGS configuration shows the minimum MAE while for the RH and WIND parameters the tUSGS-lCORINE configuration presents the minimum MAE. The MAE of MSPL lies between 1.128 and 1.131 hPa, the MAE of TEMP ranges from 1.39 to 1.4 (K), for the RH the MAE is at about 9.27-9.33 (%) and the one of WIND varies from 1.86 to 1.87 (m/s).

These differences may attributed to the fact that the HNMS station at Larissa Airport (39°38′56.76″N, 22°27′55.63″E) is the only conventional station inside the area of interest (Thessaly), among the twenty (20) available. For that reason, there is a direct feedback of the changes in topography and land-use representation at the vicinity of that station, while the remaining HNMS stations are affected indirectly, as they are located outside of the d03.

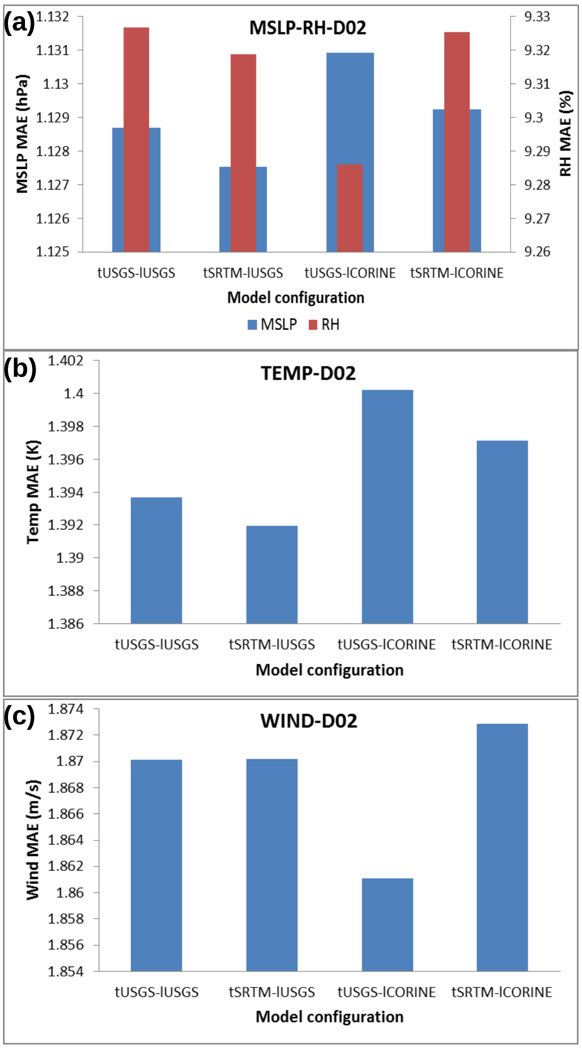

Fig. 3. The Mean Absolute Error (MAE) of (a) mean sea-level pressure and 2m relative humidity, (b) 2m air temperature and (c) 10m wind speed (d02), at the locations of the 20 HNMS stations, as a function of the four (4) model configurations.

Fig. 4 presents the Mean Absolute Error (MAE) of (a) mean sea level pressure, (b) 2m temperature, (c) 2m relative humidity and (d) 10m wind speed, at Larissa Airport (LGLR – WRF-d03), as a function of time for the four (4) topography – land-use configurations. No significant change in the MAE of MSLP variable is shown (Fig.4a) for all configurations, while the tSRTM-lUSGS configuration gives, in general, better representation of 2m temperature and 10m wind speed as a function of time. Greater MAEs are produced for the 2m relative humidity, a variable which is overestimated the most by the model.

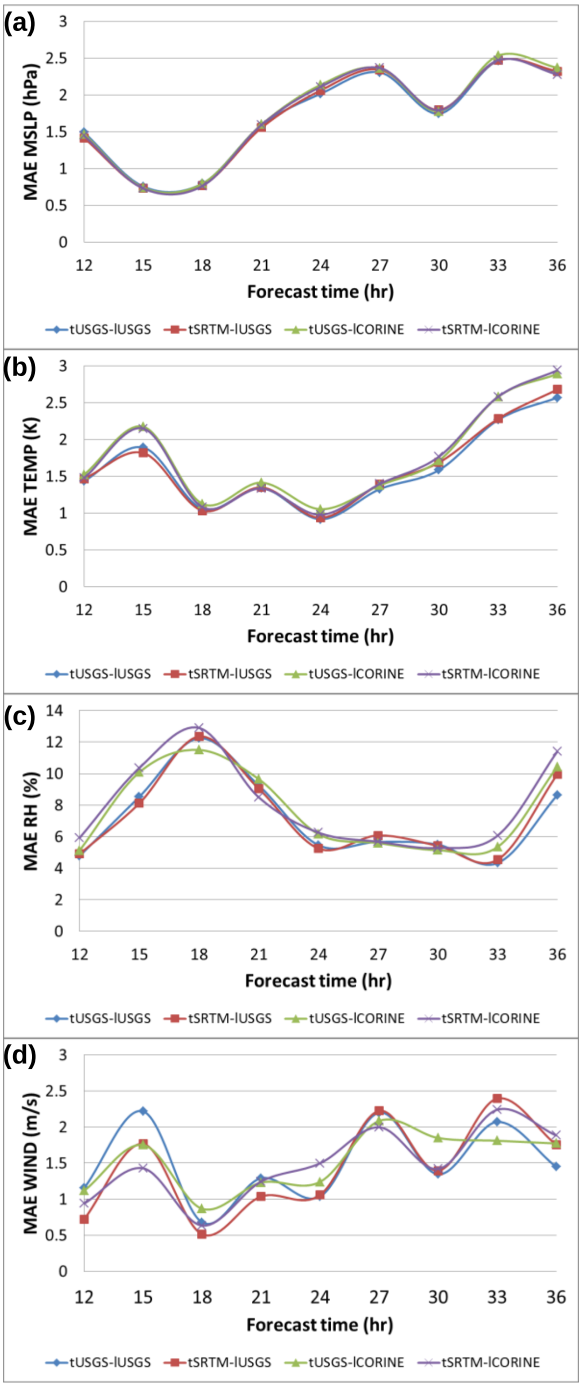

Fig. 4. The Mean Absolute Error (MAE) of a) mean sea level pressure, b) 2m temperature, c) 2m relative humidity and d) 10m wind speed, at Larissa Airport (LGLR – WRF-d03), as a function of time for the four (4) topography – land-use configurations.

Table 2 summarizes the skill scores of all topography – land-use configurations at d02. The tSRTM-lUSGS configuration shows a slightly improve of the forecast skill at d02, for MSLP, TEMP and RH parameters. The tUSGS-lCORINE configuration is less skillful than the tUSGS-lUSGS considering the MSLP and TEMP variables while the Corine land-use dataset improved the forecast skill of the control forecast regarding relative humidity and wind. The combination of the SRTM and Corine dataset (tSRTM-lCORINE) was unable to improve the overall forecast at d02 despite the better spatial representation of the topography and land-use categories at d03.

Table 2. Skill scores of all topography – land-use configurations at d02. The tUSGS-lUSGS configuration acted as control forecast for each representative day.

	tUSGS-lUSGS	*tSRTM-lUSGS*	*tUSGS-lCORINE*	*tSRTM-lCORINE*
MSLP	0.00%	0.10%	-0.20%	-0.05%
TEMP	0.00%	0.12%	-0.47%	-0.25%
RH	0.00%	0.08%	0.44%	0.01%
WIND	0.00%	0.00%	0.49%	-0.15%

3.2 The case study of 3rd of July 2009

The case of 3rd of July 2009 is presented here, as intense convective activity was occurred in the area of interest (Fig. 1b) during that day. The prevailing conditions in Greece, on 07/03/2009, corresponded to L1 (open trough) upper-air circulation type, according to Karacostas et al. (1992). Fig. 5 shows the accumulated precipitation from 00UTC 03 July to 00UTC 04 July for the area of interest (black frame in Fig1b.), as derived from radar data. From Fig. 5 it can be shown that the phenomena occurred almost in the entire region, where the maximum accumulated precipitation, for that day, exceeded 60 mm.

Fig. 6 presents the composite reflectivity (dbz), as derived from radar data and the four (4) different configurations of the WRF model, at 16UTC on 03 of July 2009. The black frame, in Fig. 6b-e, encompasses the region with radar data, which is depicted in Fig. 6a and thus the comparison is performed for that area. The model was able to capture the strength of the convective cells, at the centre of the region, in tUSGS-lUSGS (Fig. 6b), tSRTM-lUSGS, (Fig. 6c) and tSRTM-lCORINE (Fig. 6e) configurations, however there are discrepancies considering the area of the storms and their locations against the radar data. The tUSGS-lCORINE (Fig. 6d) configuration gave lower reflectivity values and weaker convective activity overall, for that particular time. Moreover, the activity which is observed in the west region of the area, in Fig. 6a, was captured by the model in all four (4) configurations, despite the spatial mismatch where the convective cells appeared mostly west and outside of the area of interest.

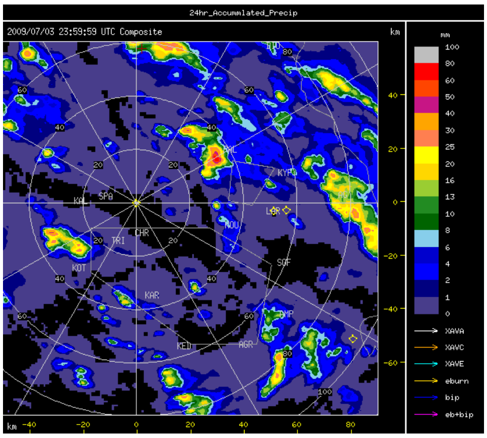

Fig. 5. Accumulated precipitation from 00UTC 03 July 2009 to 00UTC 04 July 2009, in the area of interest, as derived from radar data.

Table 3 summarizes the model errors in each configuration. WRF appears to underestimate the overall convective activity in all four (4) configurations. The convective area is underestimated the least in tSRTM-lUSGS experiment where the MAE reaches 38.48 Km^2, while in the tUSGS-lCORINE configuration is underestimated the most. Regarding the volume of the storms and the reflectivity values, the tSRTM-lUSGS setup performed quite well, with the smallest errors. In all model setups, the simulated storms were weaker than the observed ones both in intensity and area. Both cloud top and cloud base are underestimated in all four (4) setups where the maximum MAEs for cloud top and cloud base are presented in tUSGS-lUSGS run with 2.91km and 0.91km, respectively. Possible reasons for the above discrepancies include model errors, initialization errors due to the low density of conventional observations in this area, the vertical resolution of radar scan, the occurrence of the cone of silence within the area of analysis and interpolation errors during the calculation of cloud top, cloud base and volume of convective cells.

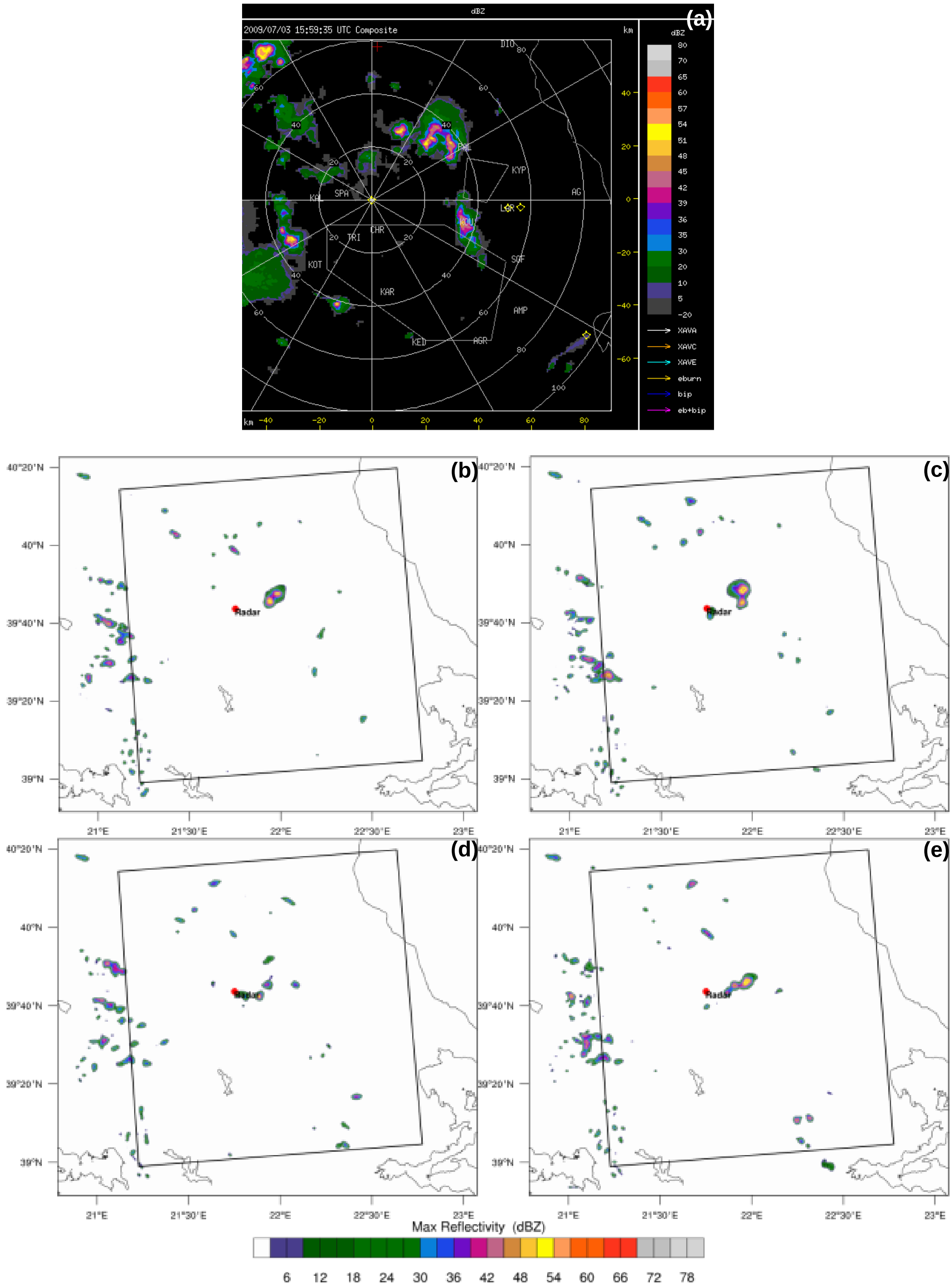

Fig. 6. Maximum reflectivity (dbz) of the column in the area of interest, at 16UTC on 03 of July 2009, for radar data (a), tUSGS-lUSGS (b), tSRTM-lUSGS (c), tUSG-lCORINE (d) and tSRTM-CORINE (e) configurations.

Fig. 7 depicts the hourly values of maximum reflectivity on 03 July 2009 for the different setups of the model against radar data. WRF modeled quite well the intensity and the time evolution of the convective event, despite the earlier prediction of the onset of activity and its termination. It should be mentioned that the radar echoes from 18UTC until the end of the day represent a single cell which developed in the southwest of the region. The model was unable to simulate that activity in all four (4) configurations. The observed radar echoes (blue markers) are in the range of about 47 to 53 dbz, while for the tUSGS-lUSGS (red markers) setup (Fig. 7a) lie between 40 to 59 dbz, for the tSRTM-lUSGS experiment (Fig. 7b) are at about 46-59 dbz, for the tUSGS-lCORINE (Fig. 7c) are from 44 to 57 dbz and for the tSRTM-lCORINE configuration (Fig. 7d) are between 42 to 57 dbz.

Table 3. Mean Error (ME) and Mean Absolute Error (MAE) of average convective area (km2), average volume (km3), maximum reflectivity (dbz), maximum cloud top (km) and average cloud base (km) for the case of 03 July 2009.

	tUSGS-lUSGS	*tSRTM-lUSGS*	*tUSGS-lCORINE*	*tSRTM-lCORINE*
		ME		
Area (km^2)	-37.30	-32.61	-39.30	-37.09
Volume (km^3)	-130.08	-115.09	-135.10	-131.89
Reflectivity (dbz)	-7.69	-5.62	-8.21	-8.88
Cloud top (km)	-0.43	-0.45	-0.95	-1.13
Cloud base (km)	-0.60	-0.63	-0.53	-0.71
		MAE		
Area (km^2)	43.69	38.48	43.27	41.09
Volume (km^3)	139.67	118.54	138.89	133.10
Reflectivity (dbz)	14.89	16.53	14.06	14.77
Cloud top (km)	2.97	2.65	2.51	2.38
Cloud base (km)	0.91	0.87	0.78	0.81

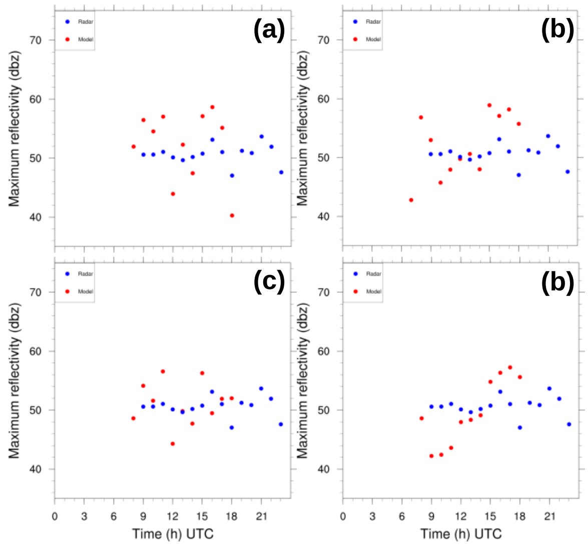

Fig. 7. Timeseries of hourly values of maximum reflectivity (at locations >= 35 dbz) on 03 July 2009, for (a) tUSGS-lUSGS, (b) tSRTM-lUSGS, (c) tUSG-lCORINE and (d) tSRTM-CORINE configurations. Blue markers represent radar measurements while red ones model values.

4. SUMMARY – CONCLUSIONS

In this study, the impact of high resolution elevation and land-use data on the convective activity over Thessaly region in Central Greece is examined through different model configurations. The use of high resolution elevation data (tSRTM-lUSGS configuration) seems to improve slightly the overall forecast (d02), in terms of mean sea level pressure, 2m temperature and 2m relative humidity while the better representation of topography in conjunction with land-use categories (tSRTM-lCORINE setup) fail to improve the overall skill score. The differences between the four (4) model configurations are very small, indicating that the changes in topography and land-use at d03, affect the overall forecast at d02 in a minor way. Current work tries to perform statistical evaluation at d03 with available surface observations.

In the area of interest, at Larissa Airport, no significant change in the MSLP's MAE is shown for all configurations, while the tSRTM-lUSGS configuration gives, in general better representation of 2m temperature and 10m wind speed for all six (6) representative cases. Greater MAEs are produced for the 2m relative humidity.

The representative case of 03 July 2009, despite some discrepancies on the onset and termination of convective activity, was simulated quite well by the model in terms of maximum reflectivity, cloud depth, average convective area and average volume of convective activity, for all configurations. However, differences occur in the intensity of the phenomena.

5. REFERENCES

Bossard, M., Feranec, J., and J. Otahel, 2000: CORINE land cover technical guide–Addendum 2000. Technical report, 40. Copenhagen (European Environment Agency, p. 105, http://terrestrial.eionet.eea.int

Dixon, M. and G., Wiener, 1993: TITAN: Thunderstorm Identification, Tracking, Analysis and Nowcasting – A radar-based methodology. J. Atmos. Ocean. Tech. 10, 785-797.

Jarvis, A., H.I. Reuter, A. Nelson and E. Guevara, 2008: Hole-filled SRTM for the globe Version 4, available from the CGIAR-CSI SRTM 90m Database (http://srtm.csi.cgiar.org).

Karacostas, T.S., A.A. Flocas, H.A. Flocas, O. Kakaliagou, and C. Rizou, 1992: A study of the synoptic situations over the area of Eastern Mediterranean, In: Proc. 1st Greek Conf. on Meteorology Climatology and Atmospheric Physics, Thessaloniki, Greece, 21-23 May, 469-477 (in Greek).

Karacostas, T., I. Pytharoulis, I. Tegoulias, E. Katragkou, and P. Zanis, 2014: Mitigating the impact of climate change on drought: the potentiality of a precipitation enhancement project (DAPHNE) in Thessaly. In: Proc. 12th Int. Conf. of Meteorology, Climatology and Physics of the Atmosphere. Heraklion, Greece, 28-31 May, 449-454.

Pineda, N., O. Jorba , J. Jorge and J. M. Baldasano (2004) Using NOAA AVHRR and SPOT VGT data to estimate surface parameters: application to a mesoscale meteorological model , International Journal of Remote Sensing, 25:1, 129-143, DOI:10.1080/0143116031000115201.

Pytharoulis, I., I. Tegoulias, S. Kotsopoulos, D. Bampzelis, S. Kartsios, P. Zanis, E. Katragkou and Th. Karacostas, 2014: High-resolution WRF hindcasts over central Greece: Characteristics of simulated convective activity and model evaluation. In Proc.: 15th Annual WRF Users' Workshop, Boulder, CO, 23-27 June.

Silverman, B.A., 2003: A Critical Assessment Of Hygroscopic Seeding Of Convective Clouds For Rainfall Enhancement. Bulletin of the American Meteorological Society, 1219-1230.

Skamarock, W.C., J.B. Klemp, J. Dudhia, D.O. Gill, D.M. Barker, M.G. Duda, X.-Y. Huang, W. Wang, and J.G. Powers, 2008: A description of the Advanced Research WRF Version 3. NCAR/TN-475.

Tegoulias, I., I. Pytharoulis, S. Kotsopoulos, D. Bampzelis, S. Kartsios, and Th. Karacostas, 2014: The influence of WRF parameterisation schemes on high resolution simulations over Central Greece. In Proc.: 15th Annual WRF Users' Workshop, Boulder, CO, 23-27 June.

The NCAR Command Language (Version 6.1.0) [Software]. (2012). Boulder, Colorado: UCAR/NCAR/CISL/VETS. http://dx.doi.org/10.5065/D6WD3XH5.

Wang, W., C. Bruyère, M. Duda, J. Dudhia, D. Gill, M. Kavulich, K. Keene, H.-C. Lin, J. Michalakes, S. Rizvi, X. Zhang, J. Beezley, J. Coen, J. Mandel, H.-Y. Chuang, N. McKee, T. Slovacek, and J. Wolff, 2013: ARW Version 3 Modeling System User's Guide. NCAR-MMM. pp. 411.

5. ACKNOWLEDGMENTS

This research is co-financed by the European Union (European Regional Development Fund) and Greek national funds, through the action "COOPERATION 2011: Partnerships of Production and Research Institutions in Focused Research and Technology Sectors" (contract number 11SYN_8_1088 - DAPHNE) in the framework of the operational programme "Competitiveness and Entrepreneurship" and Regions in Transition (OPC II, NSRF 2007-2013).